

## FABRICATION AND CHARACTERIZATION OF CR: ZNS NANOSTRUCTURES

Kamlesh Patel<sup>1</sup>, Dr. Kirti Vishwakarma<sup>2</sup>

Department of physics, Gyan Ganga Institute of Technology and Sciences Jabalpur, [M.P.] India

**Abstract:** In this paper we have employed co-precipitation technique for the fabrication of Cr: ZnS nanostructures. In this technique the structure and size of the nanostructures is controlled by altering the concentration of the dopant chromium III nitrate ( $\text{Cr}(\text{NO}_3)_3 \cdot 9\text{H}_2\text{O}$ ) and by adding suitable capping agent poly vinyl alcohol [ $\text{CH}_2\text{CH}(\text{OH})\text{Jn}$ ] (PVA) after the reaction in the solution. Fine powder of sky blue Colour Cr: ZnS nanostructures are obtained. For the characterization of nanostructures four techniques were employed. SEM gives the morphological and surface analysis of the sample at the range from 2 to 100 nm. In SEM micrograph gathering of particles could be seen clearly on increasing concentration of depent from 0.5M to 1M. XRD peaks determine that nanostructures posse's cubic structure and confirm that they have crystalline nature. FTIR pattern shows that these particles contain suitable functional group and they are in good arrangement with their constituent's particles. The analytical range employed for the sample by FTIR is from 4000 to 500nm. From 4000 to 1800nm obtained spectrum confirms the presence of chromium as a dopent replacing one of the lattice site of zinc in ZnS structure. The region from 1800 to 500 is the finger print region that confirms the presence of zinc and sulphur atom in the structure. The UV-Visible spectroscopy confirms the decrease in the band gap from 3.86 to 3.25 on increasing concentration from 0.5M to 1M.

**Keywords:** - Co-precipitation, capping agent, morphology, functional group, band gap, PVA, SEM, XRD, FTIR, UV-Visible Spectroscopy.

### I. INTRODUCTION

ZnS is one of the most important wide band gap semiconductors from II-VI group elements. Among the most studied host materials for diluted magnetic semiconductor (DMS), it means some magnetic materials with appropriate content doped in semiconducting materials known as (DMS). ZnS is a potential candidate for device applications because of its wide band gap of 3.7 eV, large exciton binding energy of 40 MeV, high index of refraction of 2.27 at 1  $\mu\text{m}$  and ZnS has been identified as an excellent host semiconductor for supporting room temperature ferromagnetism when doped with a variety of 3d transition metal ions. It is chemically more stable, nontoxic and environmentally safer than other II-VI compound semiconductors. Hence it finds more potential applications in biological detection. Doping with proper element is widely used as an effective method to tune surface states, energy levels, electrical, optical and magnetic properties of semiconducting materials. The optical and magnetic properties of doped semiconductor nanostructures are sensitive to size, morphology, crystal structure, and

effects, which may provide new opportunities for investigation and application of ZnS-based nanomaterials[1]. The zinc chalcogenides like ZnS, ZnSe and ZnTe are semiconductors with zinc blende structure at ambient conditions. The stability of high pressure phases of these zinc chalcogenides  $\text{ZnX}$  ( $X = \text{S}, \text{Se}, \text{Te}$ ) appears to be more complex. Chalcogenides such as ZnSe, ZnS have been widely used as important candidates due to their better chemical stability for photoluminescence (PL), electroluminescence (EL) cathodoluminescence (CL) and semiconductor devices. ZnS is one of the most promising luminescent materials among II-VI groups, because it exhibits wide optical transparency from the visible light of 0.4  $\mu\text{m}$  to the deep infrared region of 12  $\mu\text{m}$ . Doped ZnS semiconductor materials have a wide range of applications in phosphors, light emitting displays, optical sensors and also are used in optoelectronic applications such as reflector, dielectric filter and window materials. Efficient doping of rare-earth ions into II-VI semiconductor host is not favourable compared to the transition metals. In view of this, transition metal doped ZnS, like ZnS: Mn, ZnS: Cu, ZnS: Co and ZnS: Ni has been widely investigated. However, surprisingly, in spite of both applied and academic interest, Cr doped ZnS has been least studied. There are only a few reports on Cr doped ZnS and all these reports are on ZnS: Cr prepared by physical methods only [2]. In the present study we have chosen chemical co-precipitation route for synthesis of Cr doped ZnS nanostructures at normal temperature because this route is easy to handle, cost-effective and takes less time. The flow chart of synthesis process is given in fig.1. The prepared sample was investigated from XRD; samples were in cubical structure and highly pure. XRD patterns correspond to the (201), (111), (220) and (311) planes of diffraction peaks which belong to cubic structure. Fourier Transform Infra-Red (FTIR) Spectra confirm that Cr goes into ZnS lattice structure because atomic radius of chromium is found to be smaller than the zinc atom, so  $\text{Cr}^{+}$  ion can easily replace  $\text{Zn}^{+}$  ion from its lattice site. Scanning electron microscopy (SEM) outlines the aggregation of the particles in all samples. In the optical study it is observed that energy band gap decreases from 3.86 eV to 3.25 eV with increasing Cr concentration; blue shift in the band gap is detected. Based on density-function calculations Cr is theoretically as well as practically proposed to be a reliable dopant in ZnS. Such results on Cr doped ZnS nanoparticles are reported in this paper qualitatively and quantitatively.

### II. MATERIALS AND METHODS

Samples  $\text{Zn}_{1-x}\text{Cr}_x\text{S}$  nanoparticles were synthesized by chemical co-precipitation route at room temperature. The

starting materials were Zinc Chloride, chromium III nitrate ( $Cr(NO_3)_3 \cdot 9H_2O$ ) and sodium sulphide are of grade one. Chemicals used without further purification were of analytical grade. Distilled water is used as a solvent. The appropriate amounts of zinc chloride, chromium nitrate and sodium sulphide respectively were dissolved separately in 100 ml distilled water of desired concentration and stirred at room temperature for 2 h. Chromium nitrate solution was added into zinc chloride and stirred for 20 min. Sodium sulphide solutions then added into as prepared solutions of zinc nitrate and chromium nitrate drop wise with vigorous stirring to get homogeneous solution. Throughout the sample preparation, pH-10 of the solution was maintained. After the colour change from white to sky blue PVA is added to control the size of the particles. The light sky-blue coloured precipitate was obtained; the colour of the precipitate becomes darken as Cr concentration increases. The precipitate was continuously stirred for 2 h again to get homogeneous particle size. The precipitate was collected and washed several times by deionised water. The washed precipitate was dried at 50°C for 4 hours in the oven and ground for 15 minutes to get Cr doped ZnS nanoparticles [3].

The flow chart of preparation of Cr:ZnS nanoparticles by chemical co-precipitation is given as follows:-

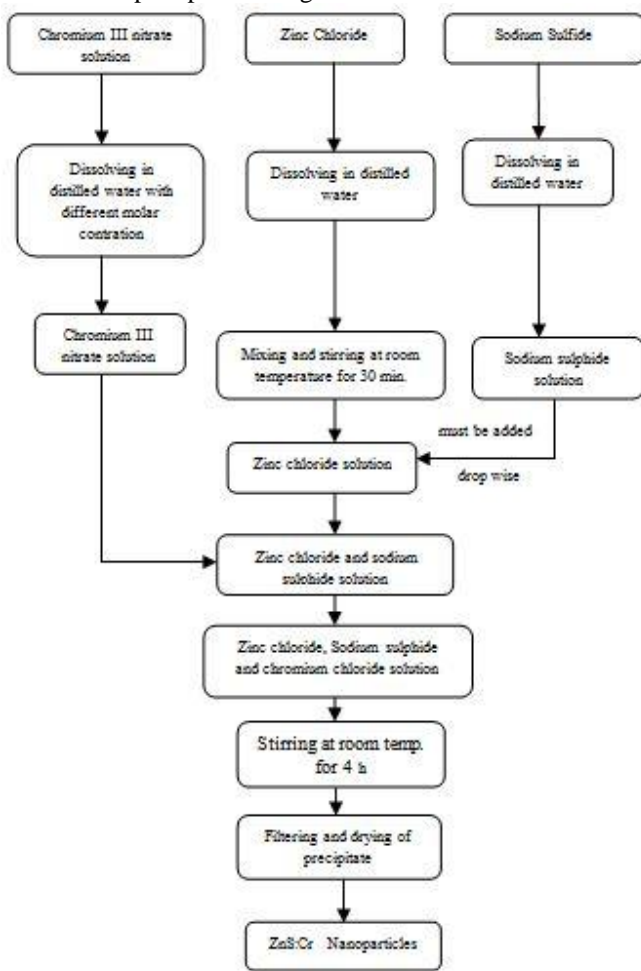


Fig. 1 The flow chart for preparation of Cr: ZnS nanoparticles by chemical co-precipitation method.

#### Characterization:

##### XRD analysis:

Data analysis: - The diffraction pattern, that includes position (angles) and intensities of the diffracted beam, provides important information about the sample. Angles are used to calculate the interplanar atomic spacing's (d-spacing's). These d spacing's (d) and intensity (I) information are used to identify the type of material by comparing them with patterns between diffracting planes of atoms determines peak position by Brag's equation ( $n\lambda=2d \sin\theta$ ).

##### Calculation of peak position by Bragg's law

$$n\lambda=2ds\sin\theta$$

Where,

$\lambda$  = wavelength

d = Inter planer Spacing.

For,  $2\theta=27^\circ$

$$d = \frac{\lambda}{2\sin\theta} = \frac{0.159\text{nm}}{2\sin(27/2)} = 1.032\text{nm}$$

X-ray diffraction for chromium shows that it has a cubic structure at wavelength of 0.154nm, one peak in the XRD pattern is at  $2\theta=27^\circ$ .

The miller indices for this peak

$$d_{hkl} = \frac{a}{(\sqrt{h^2+k^2+l^2})^{1/2}}$$

For cubic centred,  $a=2r$ .

r = Atomic radius=0.128nm

At  $2\theta=27^\circ$  and  $\lambda = 0.159\text{nm}$  it is calculated that plane lies [i.e. (111)].

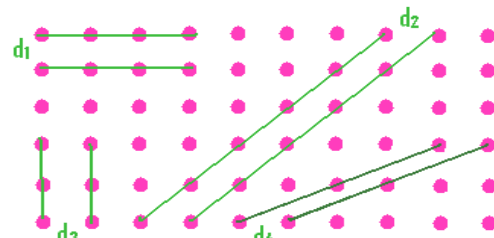


Fig. 2 Different planes in a crystal have different spacing.

The peak intensity is determined by atoms in the diffracting plane. Width of the diffracted peaks is used to determine crystallite size using Scherrer's equation.

$$t = \frac{k\lambda}{B\cos\theta}$$

Where:

t is the mean size of the ordered (crystalline) domains, which may be smaller or equal to the grain size.

K is a dimensionless shape factor, with a value close to unity. The shape factor has a typical value of about 0.9, but varies with the actual shape of the crystallite.  $K=0.9$

$\lambda$  is the X-ray wavelength.  $\lambda = 0.154\text{nm}$

B is the line broadening at half the maximum intensity (FWHM), after subtracting the instrumental line broadening, in radians. This quantity is also sometimes denoted as  $\Delta(2\theta)$ .  $B=0.5^\circ$

$\theta$  is the Bragg angle (in degrees).  $2\theta=27^\circ$

$$t = 0.9 \lambda / (B \cos \theta)$$

$$B = 0.5^\circ, \lambda = 0.154 \text{ nm}, 2\theta = 27^\circ$$

$$\theta = 13.5^\circ; \cos(13.5) = 0.972$$

$$360^\circ = 2 \times 3.142$$

$$0.5 = 0.5 \times 2 \times 3.142 / (360) = 0.00873$$

$$t = 16.3 \text{ nm}$$

If  $t = 2 \text{ mm}$  then the value for  $B$  for same reflection is

$$B = 0.9 \frac{\lambda}{t \cos \theta}$$

$$= 1.386/2 \times 10^{-3} \times 0.972 = 7.12 \times 10^{-4} \text{ radians}$$

$$7.12 \times 10^{-4} \text{ radians} = 7.12 \times 10^{-4} \times 360 / (6.284) = 0.047^\circ$$

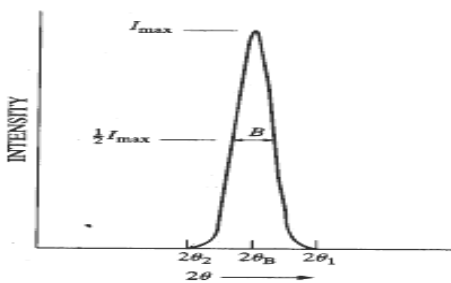


Fig. 3 FWHM and value of  $\Theta$  from peak helps in calculating crystallite size.

The X-ray diffraction (XRD) patterns of Cr:ZnS nanoparticles were recorded by Bruker system using radiation ( $\lambda=1.54184 \text{ nm}$ ) with  $2\theta$  ranging  $10\text{--}70^\circ$  and the value of  $d=1.032 \text{ nm}$ .

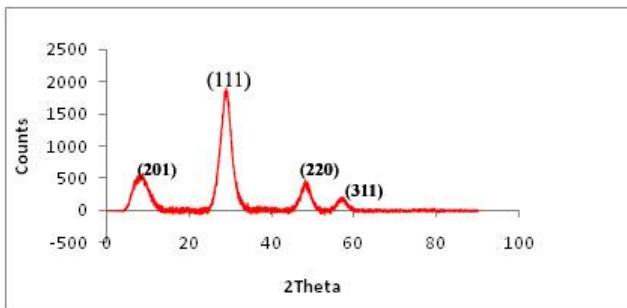


Fig. 4 XRD patterns of Cr:ZnS nanoparticles.

(Cr:ZnS)	$a (\text{nm})$	$c (\text{nm})$	FWHM( $\beta$ )	(D) nm
ZnS	0.3820	7.542	0.411	30.59
(Cr:ZnS, 0.5M)	0.3824	7.488	0.315	31.09
(Cr:ZnS, 1M)	0.3822	7.538	0.288	34.86

Table 1. The lattice parameters "a" nm, "c" nm values, average grain size (D), and FWHM ( $\beta$ ), for all the compositions of (Cr:ZnS) compound.

### III. UV-VISIBLE SPECTROSCOPY

UV-visible absorption spectroscopy involves the spectroscopy of photons in the UV-visible region. This means it uses light in the visible, near ultraviolet (UV) and near infrared (NIR) ranges. The absorption in the visible ranges directly affects the colour of the chemicals involved. In this region of the electromagnetic spectrum, molecules undergo electronic transitions. This technique is complementary to fluorescence spectroscopy, in that fluorescence deals with transitions from the excited state to the ground state, while absorption measures transitions from the ground state to the excited state [4]. The wavelength of

light that a compound will absorb is characteristic of its chemical structure. Primarily used for quantitative analysis of known compounds, UV-Vis is one of the most popular techniques in the pharmaceutical, foods and paints industries, as well as water laboratories.

### Data analysis

The UV-Absorption spectra of  $\text{Cr}_{x}\text{Zn}_{1-x}\text{S}$  samples were recorded using SHIMADZU, UV-03572 spectrometer. The prepared sample were powdered and suspended in glycerol (stirred for half an hour using magnetic stirrer for the particles to spread uniformly) and their optical absorption spectrum was recorded at room temperature over the wavelength range 200 to 800 nm.

Transmittance:  $T = I/I_0$

Absorbance:  $A = -\log_{10} T = \log_{10} I_0/I$

The Beer-Lambert Law:  $A = e.b.c$

Where the absorbance A has no units, since  $A = \log_{10} I_0/I$   
 $I_0$  is the initial radiant power

$I$  is the radiant power after light passes through sample  
 $e$  is the molar absorptivity with units of  $L \text{ mol}^{-1} \text{ cm}^{-1}$

$b$  is the path length of the sample in cm

$C$  is the concentration of the compound in solution, expressed in  $\text{mol L}^{-1}$ . The concentration of the solution is found to be 0.1M and 1M.

### Determination of energy band gap.

Band gap energy,  $E = \frac{hc}{\lambda}$

$h=6.62 \times 10^{-34} \text{ Js}$ ,  $c=3 \times 10^8 \text{ m/s}$

Therefore,  $E = \frac{1.24 \times 10^{-6}}{\lambda} \text{ eV}$ ,  $\lambda$  in meter

$E = \frac{1242.37}{\lambda} \text{ eV}$ ,  $\lambda$  in meter.

Fig.5 shows the absorption spectra of  $\text{Cr}_{x}\text{Zn}_{1-x}\text{S}$  ( $x=0.01$ ) samples. Also it is observed from the graph that the strongest absorption peak appears at about 297. The peaks which were observed in all the samples are assigned as typical internal d-d transitions of Cr ions. This attributes  $\text{Cr}^{2+}$  is incorporated at the  $\text{Zn}^{2+}$  lattice site in ZnS crystal.

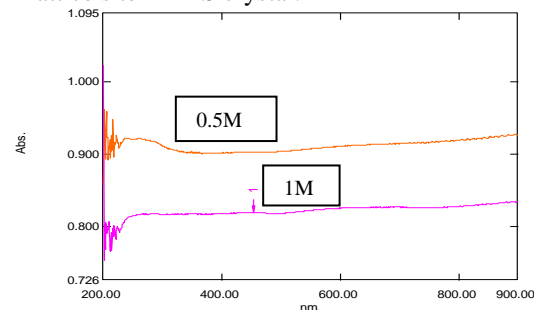


Fig. 5 UV-absorption spectra of  $\text{Cr}_{x}\text{Zn}_{1-x}\text{S}$

The fundamental absorption, which corresponds to electron excitation from the valence band to conduction band, is used to determine the value of optical band gap. The obtained band gap is decreased from 3.86 to 3.25eV with increase in Chromium concentration (x). The graphical variation of Eg with Chromium composition is shown in Fig.5. The decrease in band gap with Chromium concentration can be attributed to a real change in band strength between ZnS and CrS, change in atomic distances and grain size [5]. This result is

in agreement with the published literature. For low concentrations of Chromium, optical band gap of the material changed from 3.91-3.62 eV. By virtue of the value of their band gap they come under higher band gap materials. Therefore, they are the suitable material for fabrication of electroluminescent devices and solid state solar window layers.

Cr <sub>x</sub> Zn <sub>1-x</sub> S (x=0-0.1)	Energy band gap (Eg) eV
ZnS	3.91
Cr:ZnS(0.5M)	3.86
Cr:ZnS(1M)	3.25

Table 2. UV-absorption spectra of Cr<sub>x</sub>Zn<sub>1-x</sub>S (x=0-0.1) compound.

#### Fourier transform infrared spectroscopy (FTIR).

The FTIR studies of the samples were done by using FTIR (Make: IR Affinity-1S, SHIMADZU) in the wave number range 400-4000 cm<sup>-1</sup>. The FTIR spectrum of Cr:ZnS is shown in Fig. 6. In this spectrum the bands at 3814 cm<sup>-1</sup>, 3227 cm<sup>-1</sup> correspond to the O-H vibrations of water molecules, the peak at 2870 cm<sup>-1</sup> correspond to the C-H bond, the band at 2369 cm<sup>-1</sup> show the presence of CO<sub>2</sub> in the sample. The band at 1578 cm<sup>-1</sup> corresponds to the hydroxyl group present in the sample. The acetate bands of C-O are observed at 1215cm<sup>-1</sup>. The band at 630cm<sup>-1</sup> corresponds to the vibration of Zn-S. In this the absorption bands near 3458 cm<sup>-1</sup> represent O-H mode, those at 2956 cm<sup>-1</sup> are C-H mode, and the peaks near 1400-1700 cm<sup>-1</sup> are the C=O stretching mode. The absorption peaks at 663 cm<sup>-1</sup> corresponds to the vibrations of Zn-S. The peaks formed at 700-900 cm<sup>-1</sup> are attributed to the bond between Chromium and Sulphur. Also we can observe additional peaks in the wave number region 600-1300 cm<sup>-1</sup> which is the region of Zn-S and Cr-S bonding which again represent the presence of additional phases at higher concentration of doping. Identifying the absorbed species into the crystal surface and to confirm the formation of crystalline Cr:Zns nanoparticles. Fourier transform infrared spectroscopy study was carried out. Broad bands around 3444 cm<sup>-1</sup> and 3480 cm<sup>-1</sup> appear typically due to O-H vibrations of EDTA and water, because all FTIR spectra were carried out by mixing samples with KBr, some water vapour may be absorbed as KBr is hygroscopic. The additional weak bands and shoulders are observed at 1626 cm<sup>-1</sup> and 1639 cm<sup>-1</sup> it may be due to micro structural formation of the samples. The C-H bending of methylene in ME is observed at 1407 cm<sup>-1</sup> band. The spectra at 1149 cm<sup>-1</sup> and 1141 cm<sup>-1</sup> were observed, it due to characterization size frequency inorganic ions. The bands 1011 cm<sup>-1</sup> and 1040 cm<sup>-1</sup> observed due C-O stretching [6]. The spectra at 657 cm<sup>-1</sup> and 668 cm<sup>-1</sup> are ZnS bands that correspond to sulphide. One extra band observed in FTIR spectra for Cr concentration 0.10 at 2103 cm<sup>-1</sup> assigned due to CO<sub>2</sub> mode, it may be due to the CO<sub>2</sub> absorbed from atmosphere while doing FTIR measurements [7]. FTIR spectra of the pure and 10% Cr doped ZnS nanoparticle samples of present investigation are

in good agreement with the reported literature.

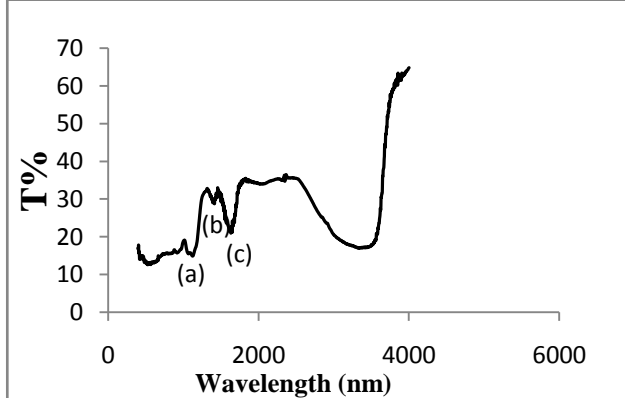


Fig .6 The FTIR spectrum of Cr:ZnS

#### Morphological study

##### SEM analysis

Scanning Electron Microscope (SEM) study is the powerful tool to study the surface morphology especially to observe the top and the cross-sectional views. Figure 7 shows the typical SEM micrographs of the Cr<sub>x</sub>Zn<sub>1-x</sub>S (x=0.5, 1.0, 1.5, 1.9) compounds. Formation of nearly spherical agglomeration in the range 100-200 nm size is evident from the micrographs. It is also noticed that, as the chromium concentration(x) increases, the morphology of the agglomerations tend to become more spherical with slight increase in the size.[8] Scanning electron microscopy was employed to get scanning electron micrographs of pure and Cr doped ZnS samples with 100 nm magnification as shown in Figure 7. It was clearly seen from SEM images that as synthesized samples exhibit the aggregation of the particles at room temperature. It is be due to the smaller particle size which is around 3 nm.

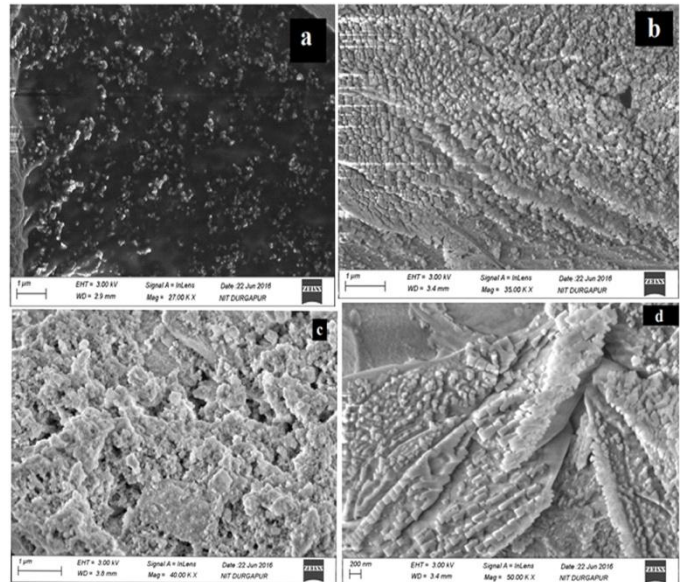


Fig. 7 SEM micrographs of pure and Cr doped ZnS nanoparticles

## IV. RESULT AND DISCUSSION

1. Cr<sub>x</sub>Zn<sub>1-x</sub>S nanoparticles were synthesized by the co-precipitation technique.
2. The XRD and SEM studies showed that Cr<sub>x</sub>Zn<sub>1-x</sub>S

compound has Polycrystalline nature and its crystallinity varied from hexagonal to near cubic with the increase in chromium concentration from ( $x=1-2M$ ) and surface properties of the compound improved by increasing chromium concentration( $x$ ).

3. XRD spectrum confirmed that the samples have cubic structure and also showed that the atomic percentages present were as per the constituents taken in the lattice site of the compound.

4. UV-Visible spectrum confirmed the decrease of band gap with increasing Chromium concentration ( $x$ ) in  $\text{Cr}_x\text{Zn}_{1-x}\text{S}$  compound.

5. The grain size in  $\text{Cr}_x\text{Zn}_{1-x}\text{S}$  has increased and dislocation density and strain values have decreased with the increase in chromium concentration ( $x$ ). And all these variations are observed to be non-linear.

6. The vibrational bands evaluated from FTIR spectra confirmed that the chromium is induced into the lattice replacing Zinc.

7. Formation of nearly spherical agglomeration in the range 100-200 nm size is evident from the SEM micrographs.

#### REFERENCES

- [1] V. Laxmi Narasimha Rao<sup>1</sup>, T. Shekharam, K. Hadasa, G. Yellaiah and M. Nagabhushanam<sup>2</sup> (2013), Synthesis and Study of Structural, Optical Properties of  $\text{Co}_x\text{Zn}_{1-x}\text{S}$  Semiconductor Compounds. IOSR Journal of Applied Physics (IOSR-JAP), e-ISSN: 2278-4861. Volume 5, Issue 1 PP 19-25.
- [2] M. R. Bodke<sup>1</sup>, Y. Purushotham<sup>2</sup>, B. N. Dole<sup>1\*</sup> (2014) Crystallographic and optical studies on Cr doped ZnS nanocrystals. 425-428.
- [3] Vishwanath Dattu Mote, Vishnu Ramrao Huse, Babasaheb Nivrutti Dole\*(2012), Synthesis and Characterization of Cr Doped ZnO Nanocrystals, World Journal of Condensed Matter Physics, 2012, 2, 208-211.
- [4] Hedayati K, Zendehnam A, Hassanpour F. Fabrication and Characterization of Zinc Sulfide Nanoparticles and Nanocomposites Prepared via a Simple Chemical Precipitation Method . J Nanostruct, 2016; 6(3):207-212.
- [5] Parvaneh Iranmanesha, Samira Saeedniab, and Mohsen Nourzpoora (2015) Characterization of ZnS nanoparticles synthesized by co-precipitation method, Chin. Phys. B Vol. 24, No. 4 (2015) 046104.
- [6] M. Romcevic, N. Romcevic, R. Kostic, L. Klopotowski, W. D. Dobrowolski, J. Kossut, And M. I. Comor, (2010) Photoluminescence of highly doped  $\text{Cd}_{1-x}\text{Mn}_x\text{S}$  nanocrystals, Journal of Alloys and Compounds, 497(1-2), 46-51.
- [7] K. Siva Kumar, A. Divya and P. Sreedhara Reddy, (2011) Synthesis and characterization of Cr doped CdS nanoparticles stabilized with polyvinylpyrrolidone, Applied Surface Science, 257(22), 9515-9518.
- [8] K. Takamura, F. Matsukura, D. Chiba and H. Hono,
- [9] (2002) Magnetic properties of  $(\text{Al},\text{Ga},\text{Mn})\text{As}$ , Applied Physics Letters, 81(14), 2590-2592.
- [10] H. Lu and S.Y. S. Chu, (2004) The mechanism and characteristics of ZnS-based phosphor powder, Journal of Crystal Growth, 265, 476-481
- [11] Alivisatos AP (1996) Semiconductor clusters, nanocrystals, and quantum dots. Sci. 271, 933-937.
- [12] Amaranatha Reddy D, Divya A, Murali G, Vijayalakshmi RP and Reddy BK (2011) Synthesis and optical properties of Cr doped ZnS nanoparticles capped by 2-mercaptopropanoethanol. Physica B. 406, 1944–1949.
- [13] Anderson MA, Gorer S and Penner RM (1997) A hybrid electrochemical/chemical synthesis of supported, luminescent cadmium sulfide nanocrystals. J. Phys. Chem. B 101, 5895.
- [14] Dios M de, Barroso F, Tojo C, Blanco MC and Lopez- Quintela MA (2005) Effects of the reaction rate on the size control of nanoparticles synthesized in microemulsions. Colloids & Surfaces A: Physicochem. Eng. Aspects. 83, 270–271.
- [15] L.D.DeLoach, R.H. Page, G.D. Wilke, S.A. Payne, S. and W.F. Krupke, (1996) “Transition metal-doped zinc chalcogenides: spectroscopy and laser demonstratio of a new class of gain media”, IEEE J. Quantum Electron 32, 885-895.
- [16] R.H.Page, K.I.Schaffers, L.D. DeLoach, G.D. Wilke, F.D. Patel, J.B. Tassano, S.A. Payne, W.F. Krupke, K.T. Chen,A. (1997) Burger,:Cr<sup>2+</sup>-doped zinc chalcogenides as efficient, widely tunable mid-infrared lasers”, IEEE J. Quantum Electron, 33/4 609-619.
- [17] K.Graham, S.B. Mirov, V.V. Fedorov, M.E. Zvanut, A. Avanesov, V. Badikov, B. Ignat'ev, V. Panyutin, G. Shevirdyaeva, (2001) “Spectroscopic characterization and laser performance of diffusion doped Cr<sup>2+</sup>:ZnS”, in Advanced Solid State Lasers, S. Payne and C. Marshall, Eds., Vol. 46 of OSA Proceedings Series (Optical Society of America, Washington, DC , p.561-567.
- [18] K..Graham, S.B. Mirov, V.V. Fedorov, M.E.Zvanut, A. Avanesov, V. Badikov, B. Ignat'ev, V. Panyutin, G. Shevirdyaeva, (2001) “Laser performance of Cr<sup>2+</sup> doped ZnS”, in Solid State Lasers X, Richard Scheps, Editor, Proc. SPIE 4267, 81-88, 2001.